A Numerical Analysis of Thermal and Shrinkage-Induced Warpage in Injection-Molded Polymer Parts

Tran-Phu Nguyen
Faculty of Energy Engineering and Transport, Ho Chi Minh City University of Technology and Engineering (HCMUTE), Vietnam
phunt@hcmute.edu.vn (corresponding author)

Thanh-Long Le
Faculty of Mechanical Engineering, Ho Chi Minh City University of Technology (HCMUT), Vietnam | Vietnam National University Ho Chi Minh City, Vietnam
ltlong@hcmut.edu.vn

Received: 12 December 2025 | Revised: 9 January 2026 and 20 January 2026 | Accepted: 23 January 2026

 DOI: https://doi.org/10.48084/etasr.16908

ABSTRACT

Warpage is a common defect in injection-molded plastic parts, leading in dimensional inaccuracy and lower product quality, so it is crucial to recognize and control warpage. This study uses simulation-based analysis with Moldex3D, an advanced injection molding simulation software, to examine the main causes of warpage. The analysis focuses on two primary factors: the temperature and the shrinkage effect. The temperature effect arises from uneven cooling rates throughout the molded component, resulting in internal thermal tensions and geometric distortion. The shrinkage effect is related to material contraction during solidification and is influenced by flow direction, wall thickness, and material characteristics. This study uses simulation to assess the impact of various processing conditions and part geometries on overall warpage. The findings show that minimizing heat gradients and controlling shrinkage distribution are important for preventing warpage, optimizing processing parameters and enhancing the dimensional stability of injection-molded plastic products.

Keywords-injection molding; warpage; temperature effect; shrinkage effect; simulation

I. INTRODUCTION

Injection molding, in spite of producing complex and high-precision components, is sensitive to various properties of the materials, leading to different kinds of defects, such as warpage. Influencing the dimensional precision and the aesthetics of the molded items, this method needs to reconsider the causes and develop effective control measures, in order to improve production efficiency and ensure the integrity of final products. Warpage is primarily caused by non-uniform shrinkage and uneven temperature distribution during the cooling and solidification stages of the injection molding process. Authors in [1] developed a three-dimensional Finite Volume Method (FVM) to simulate the mold filling phase in injection molding processes, analyzing melt flow behavior, free surface dynamics, and thermal dynamics within the mold cavity. Authors in [2] conducted a thorough review of thin-shell injection-molded parts and determined that packing pressure primarily influences warpage, followed by mold temperature, melt temperature, and packing period, emphasizing the importance of carefully controlling processing parameters to minimize warpage, particularly in components with thin walls. Authors in [3] examined the impact of gate design and material selection on warpage behavior and determined that optimal gating can substantially minimize deformation, whereas authors in [4] emphasized the importance of fiber orientation and residual stresses in fiber-reinforced polymers, demonstrating how anisotropic shrinkage results in warpage. Authors in [5] developed a numerical model to study the impact of cooling system configurations on the part's shrinkage and temperature distribution, emphasizing that the layout of cooling channels and heat exchange dynamics significantly influence polymer solidification and resulting warpage behavior. Authors in [6] studied the relationship between cooling system designs and warpage in injection-molded components, showing that variations in cooling channel design, including location and diameter, significantly affect temperature distribution throughout the mold cavity. Non-uniform cooling was identified as a primary cause of residual stresses, leading to greater warpage, highlighting the importance of optimizing cooling configurations to ensure uniform temperature distribution. Authors in [7] examined the effect of localized mold temperature control on warpage in thin-walled injection-molded components, showing that

modifying the mold temperature in specific regions stabilizes the cooling rate, eliminating residual stresses and diminishing warpage, providing an economical approach to improving the dimensional precision of molded components, particularly those with complex geometries or varying wall thicknesses. Authors in [8] demonstrated how process factors influence the strength, shrinkage, and warpage of injection-molded plastic components. Temperature, pressure distribution, and other injection parameters generate regional shrinkage, internal strains, and the relative stiffness of each part during the molding process, emphasizing the necessity of understanding the interaction between process factors and material characteristics in order to reduce warpage issues. A detailed assessment of the influence of injection molding process parameters on the strength, shrinkage, and warpage of plastic products after molding was conducted, highlighting the significance of parameters, such as melt temperature, mold temperature, injection pressure, and cooling time, in ensuring the final quality of the part. Wrong configuration of these parameters could result in significant warpage and shrinkage, affecting the dimensional accuracy and mechanical properties of the molded parts. Authors in [9] conducted a numerical analysis of warpage in lightweight hybrid products, using insert injection molding. Warpage in complicated plastic-metal hybrid components was minimized by adjusting processing settings and merging the Taguchi approach with response surface methodology. The research revealed the substantial influence of packing pressure and temperature variations at product corners on warpage, demonstrating the advantages of combining statistical and numerical methods for process optimization. Authors in [10] used a Design of Experiments (DOE) and numerical simulation to study the effect of processing parameters on warpage, confirming that packing pressure and cooling time are critical parameters. Advancements in computational tools have produced critical software, such as Moldflow and Moldex3D, for predicting warpage and other molding issues across various processing settings [11].

Authors in [12] used a combination of DOE, Response Surface Methodology (RSM), and the Firefly Algorithm (FA) to optimize processing settings and minimize warpage, showing the importance of packing time, cooling time, and melt temperature in determining warpage. Furthermore, post-molding annealing treatment significantly reduces residual stresses, leading to a substantial reduction in warpage, revealing the potential for combining process improvement with post-processing approaches to enhance the dimensional stability of injection-molded products. Authors in [13] introduced a new method for measuring warpage in injection-molded components, emphasizing the method's accuracy, ease of use, and efficiency, offering a reliable way to evaluate warpage. Authors in [14] developed a hybrid modeling methodology integrating Back Propagation Neural Networks (BPNN), Genetic Algorithms (GA), and Support Vector Machines (SVM) to predict and mitigate warpage and volume shrinkage in thin-walled injection-molded parts. This approach significantly reduced warpage and shrinkage to levels of 0.93% and 1.9%, respectively, demonstrating the potential for integrating machine learning with simulation tools to optimize processes. Authors in [15] performed a numerical simulation to evaluate the influence of various cooling channel designs on the warpage of thin-walled injection-molded components, showing that the configuration of cooling channels markedly affects the warpage behavior of molded components. Using Conformal Cooling Channels (CCCs) that closely align with the mold cavity's outlines enhances heat accumulation management within the mold, resulting in less warpage. Authors in [16] introduced a technique that minimizes warpage and cooling duration during the injection molding process by modifying the temperature differential of the coolant between the core and cavity inserts. Integrating series-connected CCCs within the core insert and parallel-connected CCCs within the cavity insert enhanced cooling efficiency by 12% at a temperature differential of 2°C. This configuration reduced average deformation by 75.2% and decreased cooling duration by 6%. Compared to traditional cooling channels, the proposed approach achieved approximately 60% improvement in deformation and 30% reduction in cooling time. Experimental validation showed that the average deformation enhancement rate was over 74.5%, and cooling time decreased by about 15.7%. Authors in [17] examined the effects of process parameters and post-molding conditions on shrinkage and warpage in injection-molded components with complex geometries. The results showed that part geometry significantly influences warpage; ribbed parts and lower holding pressures revealed increased deformation. Authors in [18] examined warpage reduction in injection-molded PA6 parts using RSM with a Box–Behnken design. They applied Moldex3D simulations and ANOVA to quantify the effects of melt temperature, mold temperature, packing pressure, and cooling time on deformation. The results confirmed that RSM efficiently determines optimal processing conditions for minimizing warpage in injection molding. A simulation-based analysis is an effective approach to understanding thermomechanical interactions during the injection molding cycle.

This study examines two primary sources of warpage—thermal and shrinkage effects—using Moldex3D, providing practical guidance to optimize mold design, processing parameters, and material selection, thereby enhancing the dimensional stability of injection-molded plastic products.

II. MATHEMATICAL MODEL

This study uses a mathematical model to examine the main cause of warpage in injection-molded plastic components. The model indicates whether deformation is primarily caused by thermal gradients (temperature effect) or material shrinkage (shrinkage effect). Figure 1 shows the modeling framework, which uses material characteristics, part geometry, and processing parameters to evaluate thermal stress formation and volumetric shrinkage during the molding process. The part under investigation is an electrical socket housing measuring 90 mm × 18 mm × 50 mm. ABS-POLYMANHH3 was chosen as the material due to its excellent dimensional stability. Thermophysical and mechanical parameters, such as viscosity, specific heat, and thermal expansion coefficients, were obtained from the Moldex3D material database. Figure 2 shows the Pressure-Volume-Temperature (PVT) diagram, which is

essential for forecasting warpage during the packing and cooling stages. The diagram clarifies the relationship between the polymer's specific volume and differences in temperature and pressure, which directly influence shrinkage behavior.

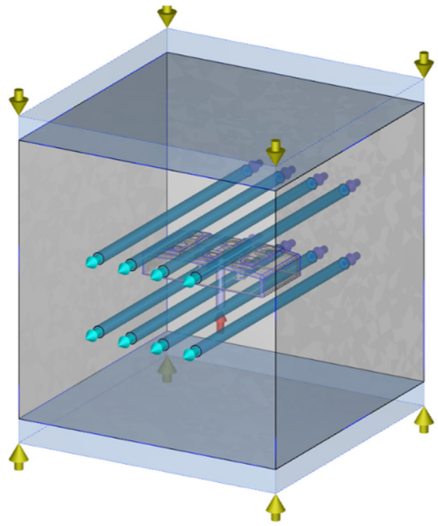

Fig. 1. Schematic diagram of the injection molding system model.

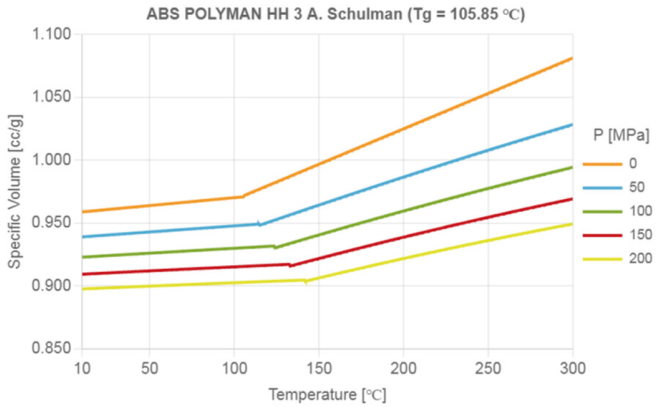

Fig. 2. The PVT diagram of ABS-POLYMANHH3.

This study examined four cases with different injection molding conditions. Case 1 (Run 1) established the original scenario, employing standard injection parameters, as displayed in Figure 3. The filling time was 1.0 s, and the packing time was 5.1 s. The melt and mold temperatures were 240 °C and 60 °C, respectively. The cooling time was 13.7 s. In Case 2 (Run 3), the gate diameter increased from 2 mm to 4 mm. In Case 3 (Run 4), the packing duration was increased from 5.1 to 7.0 s. Case 4 (Run 6) implemented both modifications: the gate diameter was increased to 4 mm and the packing duration was extended to 10.0 s. Equations (1-3) are solved using FVM:

$$\frac{\partial \rho}{\partial t}(\rho u) + \nabla \cdot (\rho u u + \tau) = -\nabla p + \rho g \quad (1)$$

$$\frac{\partial \rho}{\partial t} + \nabla \cdot \rho u = 0 \quad (2)$$

$$\rho c_p \left(\frac{\partial T}{\partial t} + u \cdot \nabla T\right) = \nabla (k \nabla T) + \eta \dot{\gamma}^2 \quad (3)$$

where ρ is the volumetric density, t is the time, u is the velocity vector, T is the temperature, p is the pressure, τ is the stress tensor, η is the viscosity, k is the thermal conductivity, C_p is the specific heat, and $\dot{\gamma}$ is the shear rate.

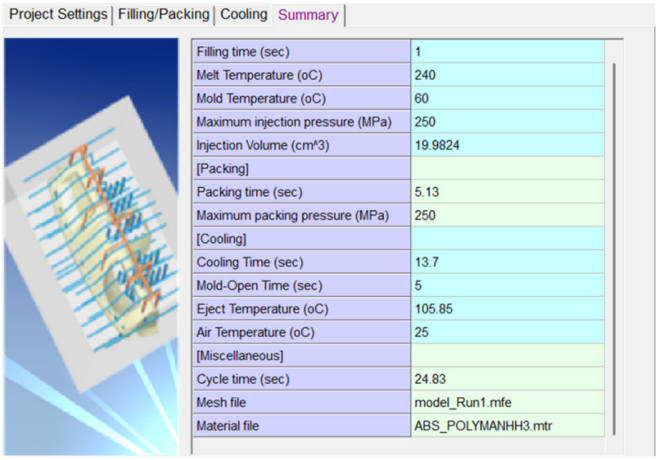

Filling time (sec)	1
Melt Temperature (oC)	240
Mold Temperature (oC)	60
Maximum injection pressure (MPa)	250
Injection Volume (cm^3)	19.9824
[Packing]	
Packing time (sec)	5.13
Maximum packing pressure (MPa)	250
[Cooling]	
Cooling Time (sec)	13.7
Mold-Open Time (sec)	5
Eject Temperature (oC)	105.85
Air Temperature (oC)	25
[Miscellaneous]	
Cycle time (sec)	24.83
Mesh file	model_Run1.mfe
Material file	ABS_POLYMANHH3.mtr

Fig. 3. The original injection molding process conditions in this study.

The following boundary condition is applied at the cavity surface:

$$n \cdot (k \nabla T) = \alpha (T_w - T_f) \quad (4)$$

where α is the convective heat-transfer coefficient, T_w is the wall temperature, and T_f is the temperature of the fluid. The outward normal vector n follows the standard sign convention for heat flux evaluations. The left side represents the conductive heat flux transferred from the mold interior to the cavity surface, whereas the right side represents the convective heat flux transferred from the hot air stream to the cavity surface. The simulation model's mesh generation used the Boundary Layer Mesh (BLM) technique from Moldex3D, detecting complicated surface and boundary flow phenomena in injection molding simulations. The BLM technique forms structured hexahedral elements near the part surfaces to ensure accurate thermal and flow boundary layer resolution, using tetrahedral elements in core areas to preserve mesh adaptability and computational efficiency. In this study, the meshing process resulted in 837,276 total elements.

III. RESULTS AND DISCUSSION

The temperature and velocity distributions of the molten polymer flow within the cavity and throughout the mold are computed and examined. Figure 4 shows the movement of the melt front during the injection molding process at four specific filling stages (25%, 50%, 75%, and 100%) to analyze flow dynamics and estimate the effect of gate positioning on uniformity of filling. At full capacity, the cavity is completely filled and all melt fronts have merged. The consistent shade and smooth contour lines indicate balanced flow with few areas of hesitation or delay. Packing pressure is essential in the injection molding process for achieving dimensional precision, minimizing shrinkage, and decreasing internal defects. During the packing phase, the pressure remains constant after the cavity is filled to compensate for the shrinkage that occurs

when the polymer cools and solidifies. This additional pressure helps ensure that molten material continues to move into areas of the mold that might otherwise develop voids or sink marks.

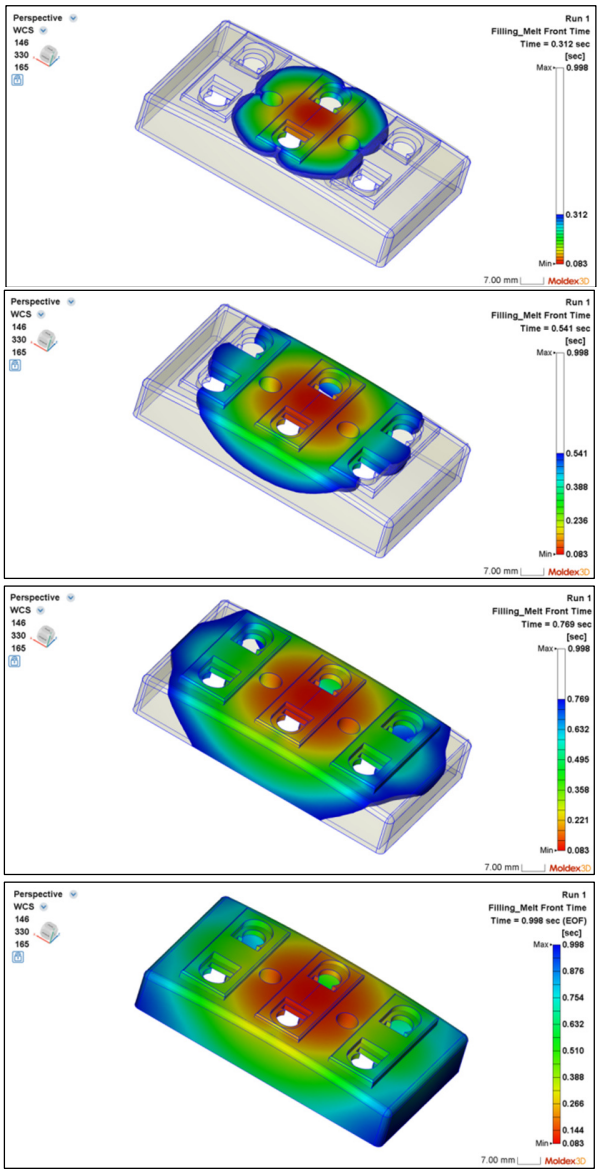

Fig. 4. Melt front time in the filling process at different stages: (a) 25%, (b) 50%, (c) 75%, and (d) 100%.

Maintaining precise control over packing pressure is essential to achieving consistent density, improving mechanical properties, and enhancing the overall quality of the molded part. Figure 5 depicts the packing pressure distribution for four different simulation situations (Runs 1, 3, 4, and 6) and demonstrates how changes in processing settings or gate designs affect internal pressure behavior at the End of Packing (EOP). These variations considerably impact the quality and dimensional stability of the molded component. The packing pressure distributions in Runs 1, 3, and 4 show significant similarities in terms of both pressure magnitude and distribution patterns.

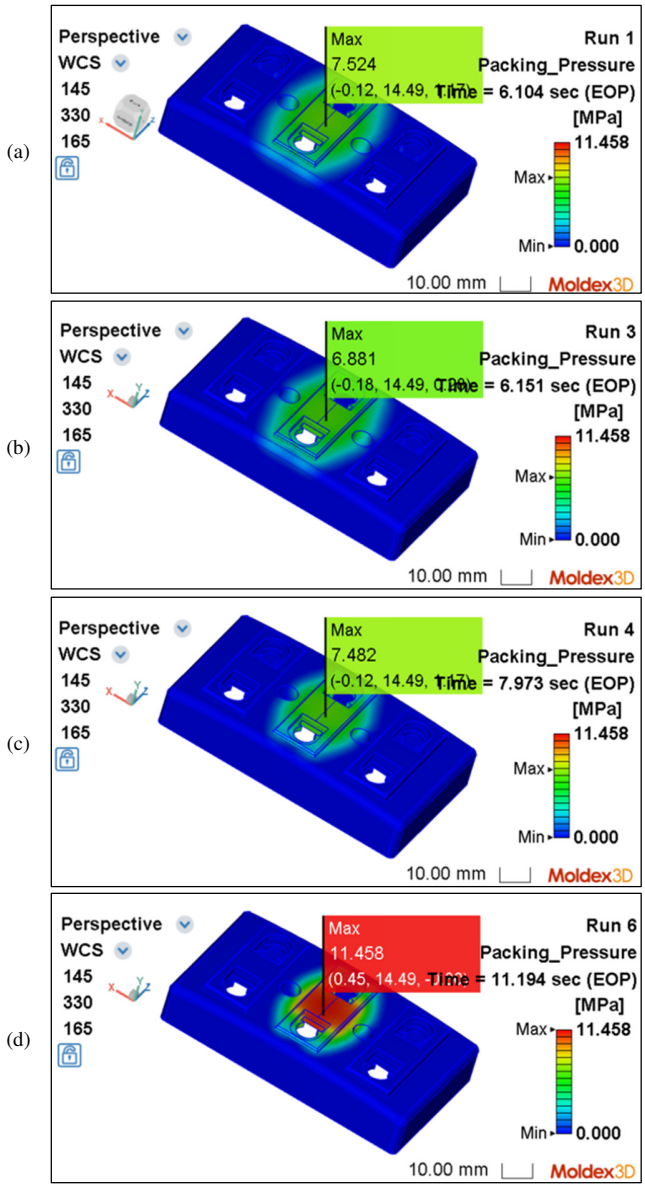

Fig. 5. The packing pressure distribution at EOP for four cases: (a) run 1, (b) run 3, (c) run 4, (d) run 6.

The maximum pressure values in all three cases are within a moderate range: 7.524 MPa in Run 1, 6.881 MPa in Run 3, and 7.482 MPa in Run 4, primarily concentrated in the gate region. This localized pressure distribution suggests an inadequate capacity to accommodate volumetric shrinkage in areas far from the gate, which can result in surface defects such as sink marks or internal voids. While there are minor differences in timing and maximum pressure values, these three cases overall indicate inadequate pressure transmission within the cavity, which could affect the dimensional accuracy and uniformity of the molded part. Conversely, Run 6 exhibits markedly enhanced results, with maximum packing pressure at 11.458 MPa, the highest recorded across all scenarios. Run 6's pressure field demonstrates a broader, more uniform

distribution, suggesting enhanced compensation for shrinkage and improved material flow during packing. These results are expected to improve dimensional stability, decrease internal stress, and enhance the surface quality of the final product.

The molten core is essential for evaluating the internal thermal condition of the molded component at the end of the packing stage. During this phase, some of the polymer material in the center of the cross-section may still be molten or semi-molten, while the outer layers have solidified due to contact with the cooler mold walls. As portrayed in Figure 6, the simulation findings indicate that Run 6 significantly deviates from the previous three cases (Runs 1, 3, and 4) due to its extended packing duration of 11.2 s.

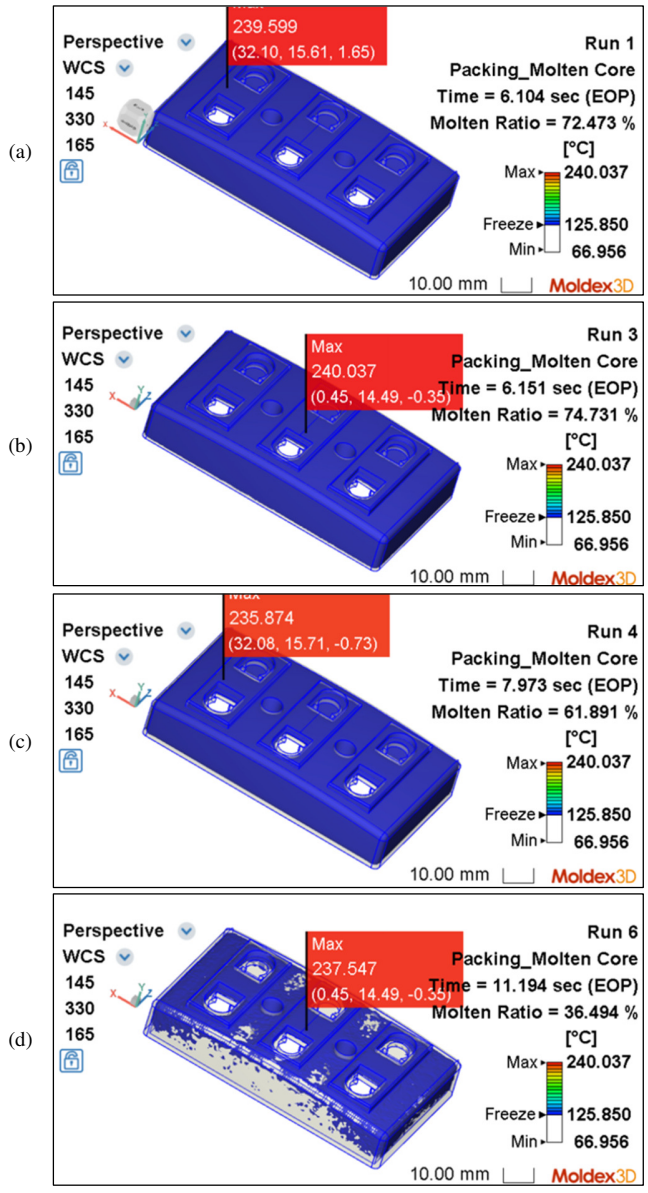

Fig. 6. The molten core at EOP distribution for four cases: (a) run 1, (b) run 3, (c) run 4, (d) run 6.

Volumetric shrinkage is the decrease in the volume of a polymer material as it cools and solidifies during and after the injection molding process. Of the four cases in Figure 7, Run 6 demonstrates better control over volumetric shrinkage due to its more efficient packing pressure. Run 6's increased and delayed packing pressure enhances compensation for material shrinkage during the packing phase. This leads to less volumetric deformation and improved dimensional stability of the molded product.

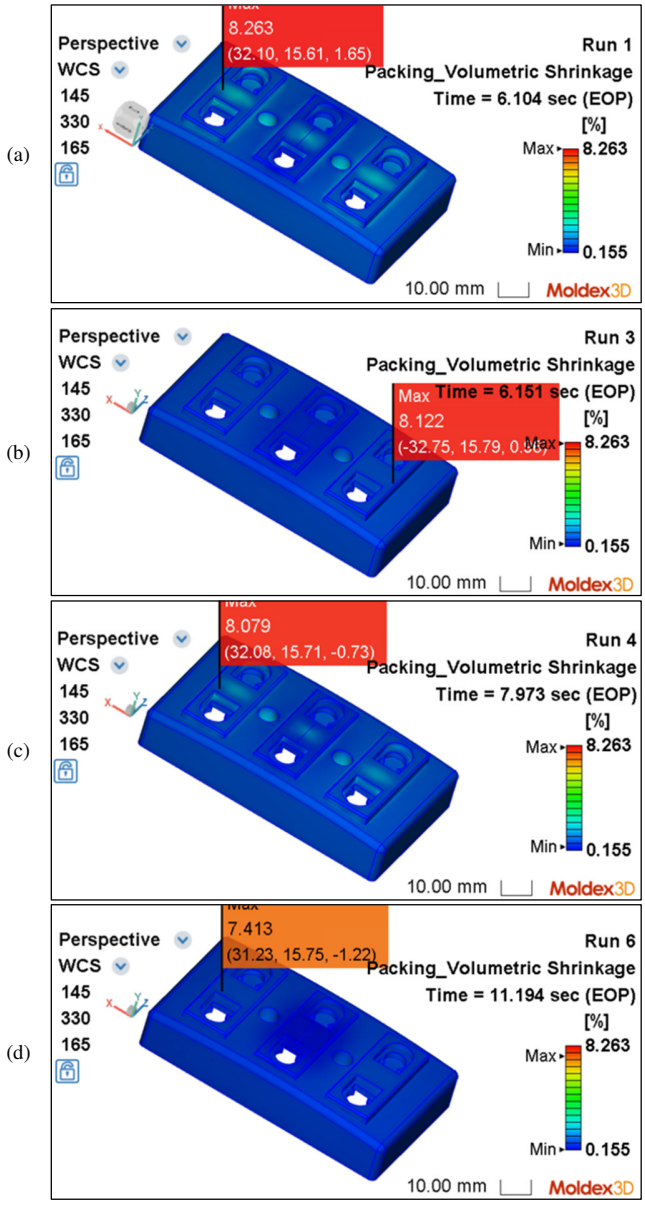

Fig. 7. The volumetric shrinkage at EOP distribution for four cases: (a) run 1, (b) run 3, (c) run 4, (d) run 6.

Figure 8 presents a statistical analysis, where Run 6 had significantly better volumetric shrinkage properties than Run 1. Run 1 had a greater maximum, average, and standard deviation of volumetric shrinkage, implying a wider and less uniform

distribution. A significant portion of the part shrank within the 4–8% range, which could lead to warpage. Run 6, on the other hand, demonstrated improved performance with reduced maximum, average, and standard deviation values of 7.413%, 2.130%, and 1.269%, respectively. Over 66% of the part volume fell within the 0.881–2.333% range, indicating more consistent shrinkage and enhanced dimensional stability.

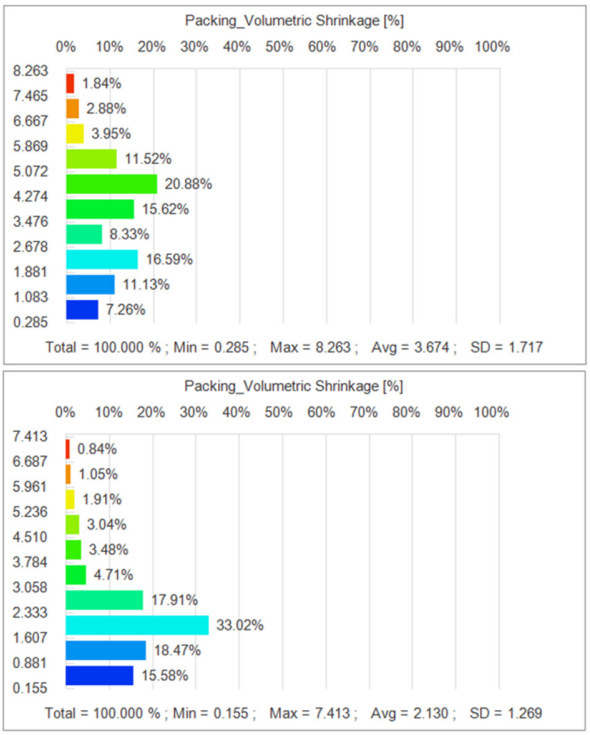

Fig. 8. The volumetric shrinkage at EOP statistics for: (a) run 1 and (b) run 6.

Figure 9 illustrates the maximum temperature distribution at the end of the cooling stage for the four cases. Run 6 has the lowest maximum temperature (170.2 °C) at the end of cooling due to its highest solidification ratio at the end of the packing phase. A greater volume of solidified material increases heat dissipation during cooling, resulting in a lower final part temperature. This improved temperature uniformity reduces residual stresses and enhances dimensional stability. Figure 10 shows that volumetric shrinkage is the predominant factor influencing overall displacement in this model, as opposed to the effects of temperature differentials. The maximum displacement resulting from shrinkage is 0.354 mm, which is significantly higher than the 0.053 mm displacement caused by temperature differentials. This suggests that internal material contraction during solidification significantly influences product deformation more than temperature gradients throughout the part do. In order to reduce warpage caused by shrinkage, it is recommended to increase packing pressure and duration, optimize gate design, promote uniform cooling, and use low-shrinkage materials. These measures enhance dimensional stability and product quality collectively. Although the temperature effect contributes minimally to overall warpage, Figure 11 demonstrates that the reduced temperature-induced displacement in Run 6 is associated with a lower maximum temperature and more uniform temperature distribution. The smaller molten core region in Run 6 suggests that more material solidifies by the end of the packing phase, eliminating internal heat gradients, thereby alleviating deformation caused by thermal contraction.

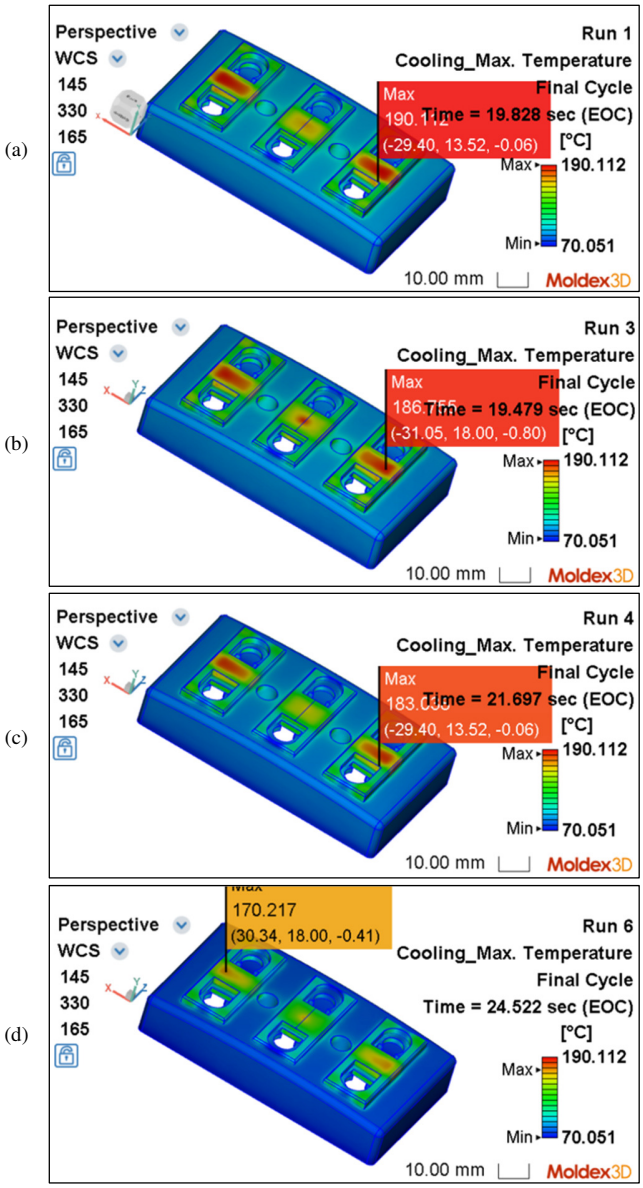

Fig. 9. The maximum temperature distribution at EOC for four cases: (a) run 1, (b) run 3, (c) run 4, (d) run 6.

Previous analyses of this model indicate that shrinkage is the primary factor influencing overall warpage behavior. Figure 12 supports this conclusion by showing the displacement distribution resulting from differential shrinkage across four separate runs. Run 6 exhibits the least shrinkage-induced displacement, with a maximum of 0.316 mm.

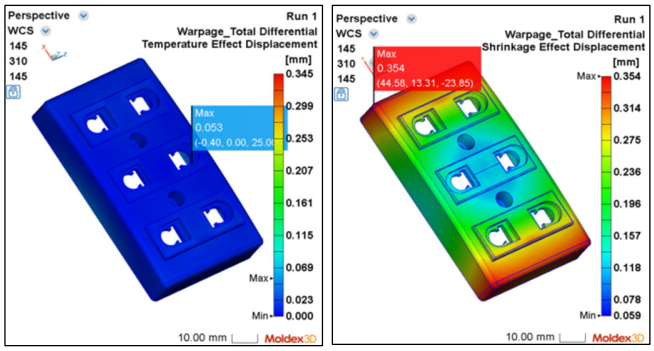

(a) (b)

Fig. 10. The contribution of : (a) the temperature effect and (b) shrinkage effect to the total displacement.

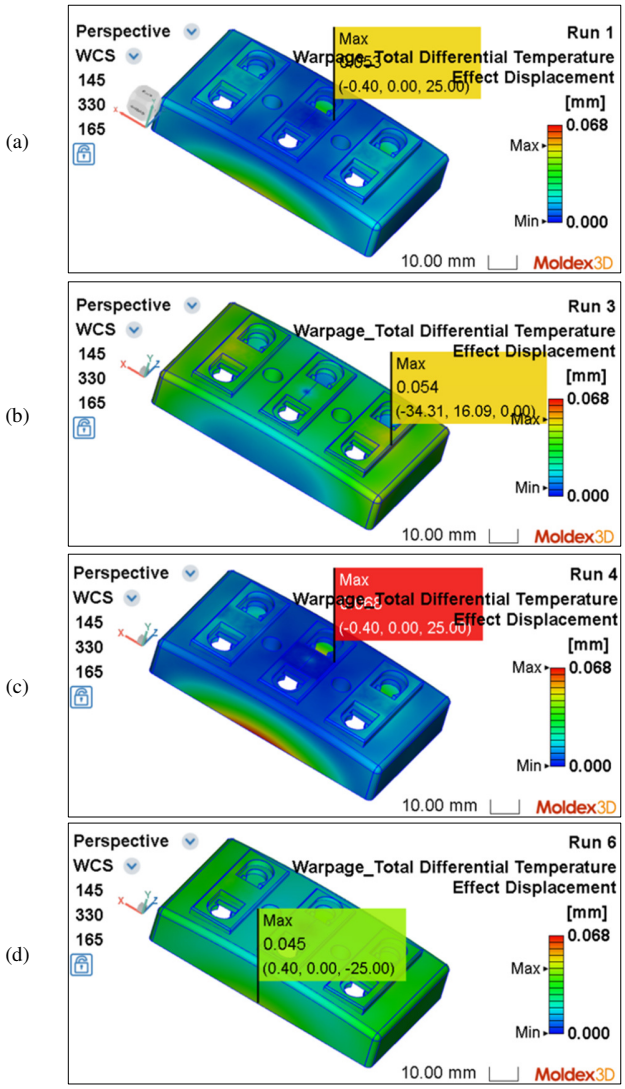

Fig. 11. The temperature effect displacement distribution for four cases: (a) run 1, (b) run 3, (c) run 4, (d) run 6.

These results highlight the importance of addressing shrinkage-related factors to improve the performance of products in injection molding processes.

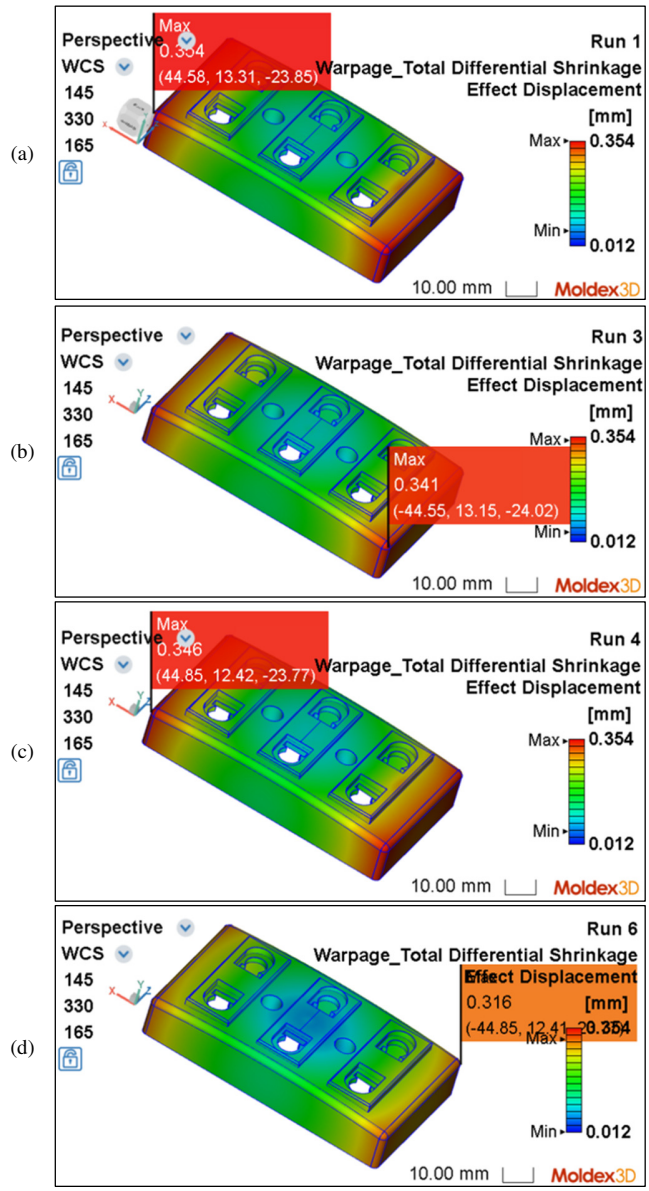

Fig. 12. The shrinkage effect displacement distribution for four cases: (a) run 1, (b) run 3, (c) run 4, (d) run 6.

This is in contrast to 0.354 mm in Run 1 and 0.346 mm in Run 4, representing a significant improvement in managing shrinkage deformation. This outcome is likely due to the improved uniformity of solidification and the optimized packing conditions in Run 6, as evidenced by the reduced molten core volume and the more uniform temperature distribution. Consequently, Run 6 can substantially reduce warpage, improving the dimensional stability and quality of the molded product.

The statistical warpage displacement distributions, shown in Figure 13, support and improve the visual analysis in Figure 12, highlighting Run 6's effectiveness in minimizing shrinkage-induced warpage. In Run 1, the peak displacement due to

shrinkage effects is 0.354 mm. This displacement is distributed broadly—7.11% of the nodes are in the upper deformation range (≥0.320 mm), and a significant portion of the model undergoes moderate-to-high displacement (16% exceed 0.286 mm). The average displacement is 0.216 mm, with a standard deviation of 0.077 mm, indicating substantial variability and an increased overall shrinking effect. Conversely, Run 6 exhibits a more favorable distribution. Notably, no nodes are present within the largest deformation range (≥0.320 mm). The mean displacement decreases to 0.190 mm, and the standard deviation decreases slightly (to 0.072 mm), indicating greater uniformity and a lower level of shrinkage deformation across the part. These results highlight Run 6's successful performance in alleviating shrinkage effects and decreasing warpage, thereby improving the dimensional uniformity and quality of the molded product.

(a)

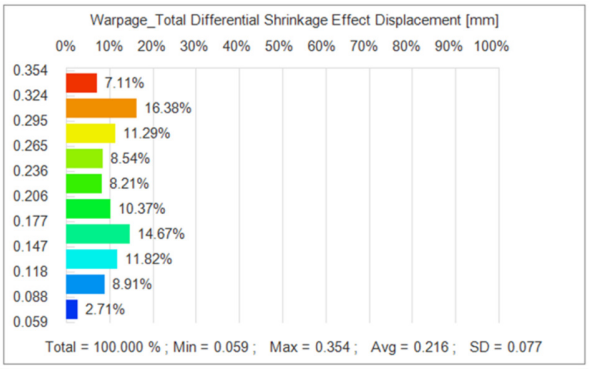

(b)

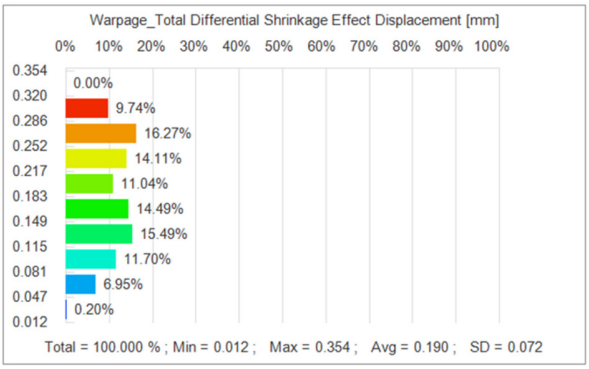

Fig. 13. The total displacement distribution statistics for: (a) run 1 and (b) run 6.

IV. CONCLUSIONS

This study used numerical simulations performed with Moldex3D to examine the primary causes of warpage in an injection-molded ABS-POLYMANNH3 electrical outlet casing. A systematic evaluation of different processing conditions was conducted to determine the relative contributions of thermal effects and material shrinkage to total deformation. The results indicate that shrinkage-induced deformation is the dominant factor governing overall warpage, while temperature has a comparatively minor influence. Run 6 exhibited the most favorable performance among the examined cases, displaying reduced molten core volume, improved temperature uniformity, and minimal shrinkage-induced displacement, leading to enhanced dimensional stability. These results underscore the importance of controlling shrinkage to reduce warpage and improve part quality in injection molding. From an industrial perspective, optimizing packing pressure and time is essential for minimizing differential shrinkage and enhancing dimensional accuracy.

ACKNOWLEDGMENT

This research is supported by Ho Chi Minh City University of Technology and Engineering (HCM-UTE), Vietnam.

REFERENCES

[1] R. Y. Chang and W. H. Yang, "Numerical simulation of mold filling in injection molding using a three-dimensional finite volume approach," *International Journal for Numerical Methods in Fluids*, vol. 37, no. 2, pp. 125–148, 2001, https://doi.org/10.1002/fld.166.

[2] M.-C. Huang and C.-C. Tai, "The effective factors in the warpage problem of an injection-molded part with a thin shell feature," *Journal of Materials Processing Technology*, vol. 110, no. 1, pp. 1–9, Mar. 2001, https://doi.org/10.1016/S0924-0136(00)00649-X.

[3] N. Zhao, J. Lian, P. Wang, and Z. Xu, "Recent progress in minimizing the warpage and shrinkage deformations by the optimization of process parameters in plastic injection molding: a review," *The International Journal of Advanced Manufacturing Technology*, vol. 120, no. 1, pp. 85–101, May 2022, https://doi.org/10.1007/s00170-022-08859-0.

[4] T.-P. Nguyen, "Effect of the Fiber Content on the Quality of the Plastic Injection Molding Product," *International Review on Modelling and Simulations (IREMOS)*, vol. 16, no. 1, pp. 20–26, Feb. 2023, https://doi.org/10.15866/iremos.v16i1.23077.

[5] H. Hassan, N. Regnier, C. Pujos, E. Arquis, and G. Defaye, "Modeling the effect of cooling system on the shrinkage and temperature of the polymer by injection molding," *Applied Thermal Engineering*, vol. 30, no. 13, pp. 1547–1557, Sept. 2010, https://doi.org/10.1016/j.applthermaleng.2010.02.025.

[6] R. Sánchez, J. Aisa, A. Martínez, and D. Mercado, "On the relationship between cooling setup and warpage in injection molding," *Measurement*, vol. 45, no. 5, pp. 1051–1056, 2012, https://doi.org/10.1016/j.measurement.2012.01.039.

[7] S.-C. Nian, C.-Y. Wu, and M.-S. Huang, "Warpage control of thin-walled injection molding using local mold temperatures," *International Communications in Heat and Mass Transfer*, vol. 57, pp. 24–30, 2015, https://doi.org/10.1016/j.icheatmasstransfer.2014.12.008.

[8] M. Mohan, M. N. M. Ansari, and R. A. Shanks, "Review on the Effects of Process Parameters on Strength, Shrinkage, and Warpage of Injection Molding Plastic Component," *Polymer-Plastics Technology and Engineering*, vol. 56, no. 1, pp. 1–12, Jan. 2017, https://doi.org/10.1080/03602559.2015.1132466.

[9] T. K. Nguyen, C. J. Hwang, and B. K. Lee, "Numerical investigation of warpage in insert injection-molded lightweight hybrid products," *International Journal of Precision Engineering and Manufacturing*, vol. 18, no. 2, pp. 187–195, 2017, https://doi.org/10.1007/s12541-017-0024-5.

[10] L. Zhang, T.-L. Chang, C.-C. Tsao, K.-C. Hsieh, and C.-Y. Hsu, "Analysis and optimization of injection molding process on warpage based on Taguchi design and PSO algorithm," *The International Journal of Advanced Manufacturing Technology*, vol. 137, no. 1, pp. 981–988, Mar. 2025, https://doi.org/10.1007/s00170-025-15099-5.

[11] J. Jiménez-Armendáriz, A. Guevara-Morales, U. Figueroa-López, M. Alfaro-Ponce, J. Martínez-Trinidad, and M. Jimenez-Martinez, "Optimization of Injection Molding Parameters for Warpage Reduction on Polypropylene Plates," *Journal of Manufacturing and Materials Processing*, vol. 9, no. 12, Dec. 2025, Art. no. 393, https://doi.org/10.3390/jmmp9120393.

[12] S. Sudsawat and W. Sriseubsai, "Warpage reduction through optimized process parameters and annealed process of injection-molded plastic parts," *Journal of Mechanical Science and Technology*, vol. 32, no. 10, pp. 4787–4799, Oct. 2018, https://doi.org/10.1007/s12206-018-0926-x.

[13] X. Sun, D. Zeng, P. Tibbenham, X. Su, and H. Kang, "A new characterizing method for warpage measurement of injection-molded thermoplastics," *Polymer Testing*, vol. 76, pp. 320–325, July 2019, https://doi.org/10.1016/j.polymertesting.2019.03.024.

[14] Z. Song, S. Liu, X. Wang, and Z. Hu, "Optimization and prediction of volume shrinkage and warpage of injection-molded thin-walled parts based on neural network," *The International Journal of Advanced Manufacturing Technology*, vol. 109, no. 3, pp. 755–769, July 2020, https://doi.org/10.1007/s00170-020-05558-6.

[15] T. P. Nguyen, T. L. Le, and T. M. T. Uyen, "Numerical Simulation on the Effect of the Cooling Channel Design on the Warpage of a Thin-Wall Injection Molding Product," *Materials Science Forum*, vol. 1075, pp. 95–101, 2022, https://doi.org/10.4028/p-8186h5.

[16] C.-C. Kuo and Y.-X. Xu, "A simple method of improving warpage and cooling time of injection molded parts simultaneously," *The International Journal of Advanced Manufacturing Technology*, vol. 122, no. 2, pp. 619–637, Sept. 2022, https://doi.org/10.1007/s00170-022-09925-3.

[17] N. B. Guerra, T. M. Reis, T. Scopel, M. S. de Lima, C. A. Figueroa, and A. F. Michels, "Influence of process parameters and post-molding condition on shrinkage and warpage of injection-molded plastic parts with complex geometry," *The International Journal of Advanced Manufacturing Technology*, vol. 128, no. 1, pp. 479–490, Sept. 2023, https://doi.org/10.1007/s00170-023-11782-7.

[18] V.-L. Trinh, "Reducing Warpage of Injection Molding Products using Response Surface Methodology," *Engineering, Technology & Applied Science Research*, vol. 15, no. 3, pp. 22355–22359, June 2025, https://doi.org/10.48084/etasr.10495.